British Journal of Pharmacology

DOI:10.1111/j.1476-5381.2012.02197.x
www.brjpharmacol.org

RESEARCH PAPER

Receptor activity-modifying protein-dependent impairment of calcitonin receptor splice variant Δ(1–47)hCT$_{(a)}$ function

T Qi[1], M Dong[2], HA Watkins[1], D Wootten[3], LJ Miller[2] and DL Hay[1,4]

[1]*School of Biological Sciences, University of Auckland, Auckland, New Zealand,* [2]*Department of Molecular Pharmacology and Experimental Therapeutics, Mayo Clinic, Scottsdale, AZ, USA,* [3]*Drug Discovery Biology, Monash Institute of Pharmaceutical Sciences and Department of Pharmacology, Monash University, Parkville, Vic., Australia, and* [4]*Maurice Wilkins Centre of Research Excellence for Molecular Biodiscovery, University of Auckland, Auckland, New Zealand*

Correspondence
Debbie L Hay, School of Biological Sciences, University of Auckland, Thomas Building, 3A Symonds Street, Private Bag 92019, Auckland 1142, New Zealand. E-mail: dl.hay@auckland.ac.nz

Keywords
amylin; calcitonin; G-protein coupled receptor; receptor activity-modifying protein; RAMP; splice variant

Received
3 July 2012
Revised
7 August 2012
Accepted
10 August 2012

BACKGROUND AND PURPOSE

Alternative splicing expands proteome diversity to GPCRs. Distinct receptor variants have been identified for a secretin family GPCR, the calcitonin receptor (CTR). The possible functional contributions of these receptor variants are further altered by their potential interactions with receptor activity-modifying proteins (RAMPs). One variant of the human CTR lacks the first 47 residues at its N terminus [Δ(1–47)hCT$_{(a)}$]. However, very little is known about the pharmacology of this variant or its ability to interact with RAMPs to form amylin receptors.

EXPERIMENTAL APPROACH

Δ(1–47)hCT$_{(a)}$ was characterized both with and without RAMPs in Cos7 and/or HEK293S cells. The receptor expression (ELISA assays) and function (cAMP and pERK1/2 assays) for up to six agonists and two antagonists were determined.

KEY RESULTS

Despite lacking 47 residues at the N terminus, Δ(1–47)hCT$_{(a)}$ was still able to express at the cell surface, but displayed a generalized reduction in peptide potency. Δ(1–47)hCT$_{(a)}$ retained its ability to interact with RAMP1 and formed a functional amylin receptor; this also appeared to be the case with RAMP3. On the other hand, its interaction with RAMP2 and resultant amylin receptor was reduced to a greater extent.

CONCLUSIONS AND IMPLICATIONS

Δ(1–47)hCT$_{(a)}$ acts as a functional receptor at the cell surface. It exhibits altered receptor function, depending on whether it associates with a RAMP and which RAMP it interacts with. Therefore, the presence of this variant in tissues will potentially contribute to altered peptide binding and signalling, depending on the RAMP distribution in tissues.

Abbreviations

AM, adrenomedullin; Amy, amylin; AMY, amylin receptor phenotype; CT, calcitonin; CTR, calcitonin receptor; CGRP, calcitonin gene-related peptide; CLR, calcitonin receptor-like receptor; RAMP, receptor activity-modifying protein

Introduction

GPCR mRNA splicing with its resultant changes to receptor sequence adds considerable potential diversity to cellular responses by altering receptor pharmacology and signalling. The secretin family of GPCRs is only a small family of 15 members, yet their capacity to contribute to a diverse array of functions is expanded through distinct receptor splice vari-

ants and interactions with receptor activity-modifying proteins (RAMPs) (Hay *et al.*, 2006; Furness *et al.*, 2012). Different combinations of RAMPs and receptor splice variants could generate many unique phenotypes that fine-tune physiological responses. One receptor that exemplifies this is the calcitonin (CT) receptor (CTR).

CT is a 32-amino acid hormone that modulates calcium homeostasis through inhibiting osteoclast-mediated bone resorption (Sexton *et al.*, 1999; Pham *et al.*, 2005). CT is well-known to enhance bone stability and has been widely used for the treatment of bone disorders. For instance, salmon (s) CT (e.g. Miacalcin, Novartis, Basel, Switzerland) is an approved drug for treating osteoporosis. Its receptor, CTR, accommodates a seven-transmembrane helical structure with a long extracellular N terminus (~150 amino acids), a prominent characteristic of the secretin family GPCRs. Several CTR splice variants have been described in humans, with others existing in different species (Furness *et al.*, 2012). These include a truncated CTR variant isolated from human breast carcinoma MCF-7 cells (Albrandt *et al.*, 1995). The receptor is the leucine 447 polymorphic insert negative variant human (h) $CT_{(a)}$, lacking the 16-amino acid insert in the first intracellular loop with an additional truncation of the first 47 amino acids in its N terminus [$\Delta(1–47)hCT_{(a)}$]. This truncation contains the predicted signal sequence of 22 amino acids and one of the four potential N-linked glycosylation sites (Ho *et al.*, 1999). The N terminus of the secretin family GPCRs is the initial docking site for their peptide ligands and the extreme N terminus of CTR is thought to contain contact points for CT (Dong *et al.*, 2004a,b; Pham *et al.*, 2004; 2005). Tissue distribution analysis identified the transcript of this truncated $hCT_{(a)}$ variant in various human tissues, including kidney, skeletal muscle, lung, both the caudate nucleus and the hypothalamus regions of the brain, whole brain and fetal brain (Albrandt *et al.*, 1995). It was also faintly visible in the pancreas but not in SK-N-MC neuroblastoma or U-2 OS osteogenic sarcoma cell lines.

CTR can also associate with RAMPs (RAMP1, RAMP2 or RAMP3) and act as pharmacologically distinct receptors for amylin (Amy): the AMY_1, AMY_2 and AMY_3 receptors (Poyner *et al.*, 2002). The abbreviation Amy denotes the peptide, but AMY denotes the receptor complex for this peptide. Amy and CT are related peptides, both belonging to the CT family of peptides, which also includes the calcitonin gene-related peptides (CGRPs), adrenomedullin (AM) and AM2. Interestingly, CGRP and Amy are equipotent at the AMY_1 receptor; the physiological relevance of this receptor to the actions of either peptide is still unknown (Hay *et al.*, 2005).

Amy was initially discovered in amyloid deposits of human insulinoma and the pancreas of type 2 diabetic patients (Cooper *et al.*, 1987). This peptide inhibits gastric emptying, gastric acid secretion, postprandial glucagon secretion and food intake (Guidobono *et al.*, 1994; Young *et al.*, 1995; Fineman *et al.*, 2002; Mack *et al.*, 2007). Symlin™ (Amylin Pharmaceuticals, San Diego, CA, USA), a modified form of human Amy, is commercially available for the treatment of type 1 and type 2 diabetes.

Despite the physiological and therapeutic relevance of CT and Amy, how they interact with their receptors is still poorly understood and there is still much to be learnt about the potential contribution of CTR splice variants to their biology. In particular, very limited work has been carried out with the truncated $hCT_{(a)}$ variant and it is not known whether this receptor retains its ability to interact with RAMPs. Given that the extreme N terminus of the closely related receptor, calcitonin receptor-like receptor (CLR), is involved in RAMP1 interactions, CTR association with RAMPs could be reduced in the truncated CTR variant (Ittner *et al.*, 2005; Haar *et al.*, 2010). As RAMP association is needed for high affinity Amy binding, this CTR splice variant could act as a natural regulator of AMY receptor function in some cells. Therefore, we hypothesized that $\Delta(1–47)hCT_{(a)}$ has different pharmacology from CTR due to changes in RAMP association and/or loss of peptide contact points. Distinct receptor phenotypes were observed depending on which RAMP $\Delta(1–47)hCT_{(a)}$ was co-expressed with. These effects appeared to be independent of changes in RAMP expression.

Methods

Materials

Untagged $hCT_{(a)}$ (leucine polymorphic variant) was kindly provided by Sebastian Furness (Monash University, Melbourne, Victoria, Australia). hRAMP1 with an N terminal myc tag (mychRAMP1) and hRAMP3 were kindly provided by Steven Foord (GlaxoSmithKline, Stevenage, UK) and have been previously described (Qi *et al.*, 2008). hαCGRP, hβCGRP, Tyr°hαCGRP, rat (r) Amy, hCT, sCT, AC187 and $sCT_{8–32}$ were purchased from American Peptide (Sunnyvale, CA, USA) or Bachem (Bubendorf, Switzerland). Anti-CTR MAb 9B4 was initially provided as a gift by Peter Wookey (University of Melbourne, Melbourne, Victoria, Australia) and later purchased (Welcome Receptor Antibodies Pty Ltd, Melbourne, Victoria, Australia). Anti-c-myc antibody was purchased from Calbiochem (San Diego, CA, USA). Anti-HA antibody was purchased from Covance (Princeton, NJ, USA). An anti-FLAG antibody was purchased from Sigma-Aldrich (Saint Louis, MO, USA). IBMX, BSA, PKA and activated charcoal were from Sigma (St. Louis, MO, USA). DMEM and FBS were from Invitrogen (Carlsbad, CA, USA). Forskolin was from Tocris (Bristol, UK). All other reagents were of analytical grade.

Generation of $\Delta(1–47)hCT_{(a)}$ construct

An $hCT_{(a)}$ construct [$\Delta(1–47)hCT_{(a)}$] which has identical amino acid sequence to the truncated isoform identified in tissues by Albrandt *et al.* (1995) was generated. There is an internal EcoRI restriction site in the cDNA sequence of $hCT_{(a)}$ corresponding to residue N194. To remove residues 1–47 from the full-length $hCT_{(a)}$, the cDNA sequence encoding receptor fragment M48-N194, which contained a HindIII restriction site at the start, was amplified by PCR and ligated to the pcDNA3 vector containing $hCT_{(a)}$ (proline polymorphic variant) cDNA that had been digested by both HindIII and EcoRI to remove the cDNA sequence encoding M1-N194. Sequence analysis of the truncated $hCT_{(a)}$ variant identified by Albrandt *et al.* (1995) shows that the receptor is a leucine polymorphic variant at position 447 and also contains an isoleucine to threonine mutation at position 347. Therefore, forward and reverse oligonucleotide primers were designed with single base changes to incorporate amino acid point mutations at positions 347 (I347T) and 447 (P447L) in the

mutant construct with residues 1–47 truncated. This method has previously been described (Bailey and Hay, 2007). Δ(1–47)$hCT_{(a)}$ with I347 was also used in some experiments as specified. All primers were custom-synthesized by Integrated DNA Technologies (Interleuvenlaan, Leuven, Belgium).

Generation of FLAG RAMPs

The sequence corresponding to the FLAG epitope was incorporated into the N terminus of RAMP1, RAMP2 and RAMP3 cDNA to introduce the FLAG tag at positions 24, 42 and 25, respectively, in the final protein. This was achieved using overlap extension PCR (Higuchi *et al.*, 1988), thereby generating PCR products for each of the FLAG-tagged RAMPs with flanking restriction sites HindIII and XbaI. Briefly, two PCR products were generated for each RAMP. The first consisting a portion of pcDNA3 including a HindIII restriction sequence, the N terminal portion of the RAMP (prior to insertion of epitope tag) and the FLAG sequence using primers T7 and P2 (Supporting Information Table S1). The second PCR product was generated using primers P3 (Supporting Information Table S1) and BGH and contained the FLAG epitope sequence followed by the remaining RAMP (corresponding to residues 25, 43 and 26 onwards in RAMPs 1, 2 and 3, respectively) and a portion of pcDNA3 including an XbaI restriction site. A third PCR was performed using primers T7 and BGH with the template consisting of a 1:1 molar ratio of the PCR products generated from the previous two reactions. This produced a final PCR product consisting of the final RAMP construct with FLAG epitope incorporated into the required position flanked by the two restriction sites. PCR products were digested using HindIII and XbaI and ligated into pcDNA3 (which had been cut with the same restriction enzymes). Sequences were confirmed by automated fluorescent sequencing (Australian Genome Resource Facility, Melbourne, Australia).

Cell culture and transfection

Both Cos7 and HEK293S cells were cultured in DMEM supplemented with 8% heat inactivated FBS and 5% v/v penicillin/streptomycin and kept in a 37°C humidified 95% air/5% CO_2 incubator. Cells were seeded into 96 well plates 1 day prior to transfection. Ninety-six well plates seeded with HEK293S cells were pre-coated with 1.5 μg of poly-D-lysine per well prior to use. Cells were transiently transfected using polyethylenimine as described previously (Bailey and Hay, 2006). Cells were used for experimentation 36–48 h later.

Cell-surface expression by ELISA

Cell-surface expression of Δ(1–47)$hCT_{(a)}$ and $hCT_{(a)}$ in the absence and presence of mychRAMP1, FLAGhRAMP1 or FLAGhRAMP2 was assessed by measuring $hCT_{(a)}$, mychRAMP1, FLAGhRAMP1 or FLAGhRAMP2 expression using whole-cell ELISA. The method has been previously described (Bailey and Hay, 2007). The anti-CTR MAb 9B4 antibody, myc antibody and FLAG antibody were used at a dilution of 1:500, 1:250 and 1:1500 respectively.

cAMP assays

cAMP assays were performed as described previously (Bailey and Hay, 2006). Briefly, transfected cells were serum-deprived in DMEM containing 1 mM IBMX and 0.1% BSA for 30 min before addition of agonists (rAmy, hCT, sCT, hαCGRP, hβCGRP or Tyr°hαCGRP) and incubation at 37°C for 15 min. cAMP was extracted with absolute ethanol and measured. For antagonist experiments (AC187 and $sCT_{8–32}$), intracellular cAMP accumulation was measured for rAmy in the absence and presence of three antagonist concentrations (1 μM, 100 nM and 10 nM).

ERK1/2 phosphorylation assays

Transfected Cos7 cells were serum-deprived in DMEM containing 0.1% BSA at 37°C overnight. The length of time between transfection and assay was the same in both cAMP and ERK1/2 assays. The cells were then stimulated with agonists (rAmy or hCT) at 37°C for 7 min (determined as optimal in a time course experiment, not shown). After incubation, the contents of the wells were aspirated and 30 μL of lysis buffer was added as per the AlphaScreen SureFire pERK1/2 kit protocol (PerkinElmer Life and Analytical Sciences, Waltham, MA, USA). The plate was gently shaken at room temperature for 10–15 min. Five microlitres of cell lysates per well was transferred to a white 384-well opti-plate, followed by the addition of 7 μL of reaction mix to each well. The plate was sealed and incubated in the dark for 2 h at room temperature. The plate was then read using an Envision plate reader (PerkinElmer Life and Analytical Sciences).

HEK293S PCR

Total RNA was extracted from cultured HEK293S cells in a T75 cm^2 flask at approximately 80% confluency. Untransfected cells were harvested and TRIZOL® Reagent (Invitrogen) was used to extract genomic RNA according to the manufacturer's instructions. cDNA was synthesized using Superscript™ first strand synthesis system (Invitrogen) as previously described (Bailey and Hay, 2006). PCR was carried out as previously described (Bailey and Hay, 2006) using primers for human RAMP1, 2 and 3 and human CTR and CLR. Primers for the human housekeeping gene – GAPDH CCAC CCATGGCAATTCCATGGCA (forward) and TCTAGACG GCAGGTCAGGTGGAGG (reverse) – were used as a positive control. The negative control contained no DNA template. PCR was carried out at an annealing temperature of 58°C for all reactions, except GAPDH, which used an annealing temperature of 50°C. PCR cycling consisted of a hot start of 95°C for 2 min, followed by 35 cycles at the requisite annealing temperature for 30 s and an extension step of 72°C for 30 s. A final extension step was carried out at 72°C for 10 min. All PCR products were then run on a 2% agarose gel using SYBR Safe™ (Invitrogen) to visualize the PCR products.

Data analysis

Data were analysed using GraphPad Prism (version 5.01, GraphPad Software Inc., San Diego, CA, USA). cAMP data were normalized to the response obtained to 50 μM forskolin that was present as a control on each plate. ERK1/2 phosphorylation data were normalized to the response elicited by stimulation with 50% FBS. For agonist responses, data were fitted to obtain concentration–response curves using a four-parameter logistic equation. *F*-test was conducted to compare if the Hill slope of the curves was significantly different from 1. In most analyses, the Hill slope was not different from 1

and was therefore constrained to 1. pEC_{50} and E_{max} values were obtained from the concentration–response curves and compared between receptors using unpaired *t*-tests.

For calculation of antagonist potency in cAMP assays, agonist concentration–response curves in the absence and presence of antagonist were fitted using global Schild analysis (Hay *et al.*, 2005). After confirming that the slope was not significantly different from 1, it was constrained to 1. The resulting estimate of pA_2 represents the pK_B (Neubig *et al.*, 2003). Unpaired *t*-tests were used to compare data.

In ELISA, expression values were normalized to wild-type (WT) expression levels as 100% and pcDNA3 alone as 0%. For receptor expression determined using RAMPs, data are expressed as a percentage of $hCT_{(a)}$/mychRAMP1, $hCT_{(a)}$/FLAGhRAMP1 or $hCT_{(a)}$/FLAGhRAMP2 expression, while $hCT_{(a)}$ alone expression was used when measured by anti-CTR 9B4 antibody. After this normalization, the mean values of all the replicates from each experiment were combined. All data were compared using one-way ANOVA, followed by Dunnett's test for comparisons between the truncated and WT receptors, or Tukey's test for multiple comparisons. In all analyses, significance was achieved at $P < 0.05$.

Results

AMY receptor pharmacology is known to be affected by cellular background, particularly for $AMY_{2(a)}$ receptors (Tilakaratne *et al.*, 2000; Hay *et al.*, 2005; Qi *et al.*, 2008). Therefore, we used both Cos7 and HEK293S cells for this study. We have previously shown that our Cos7 cells lack endogenous RAMPs, CLR or CTR (Bailey and Hay, 2006) and herein confirm that this is also the case for our HEK293S cells (Supporting Information Figures S1 and S2).

Cell-surface expression

A specific anti-CTR antibody (9B4) (Wookey *et al.*, 2012) recognizing the N terminus of CTR beyond residue 47 was used to determine the cell-surface expression of $\Delta(1–47)hCT_{(a)}$ and $hCT_{(a)}$ both alone or in complex with RAMPs. $hCT_{(a)}$ is required for the efficient translocation of RAMPs to the cell surface; therefore, RAMP expression was measured to provide an estimation of RAMP/CTR association and cell-surface expression of the AMY receptor complexes (Christopoulos *et al.*, 1999).

$\Delta(1–47)hCT_{(a)}$ expression was either slightly enhanced (Cos7) or significantly reduced (HEK293S) compared with full-length $hCT_{(a)}$, depending on the cellular background (Figure 1A). In Cos7 cells, mychRAMP1 cell-surface expression was significantly reduced when expressed with $\Delta(1–47)hCT_{(a)}$ compared with $hCT_{(a)}$ (Figure 1A). To confirm that the reduction observed with mychRAMP1 was not a result of a specific tag used in the hRAMP1 construct, another tagged version of hRAMP1, FLAGhRAMP1, was used to estimate $AMY_{1(a)}$ expression in Cos7 cells. Similar observations were seen with FLAGhRAMP1 in Cos7 cells where FLAGhRAMP1

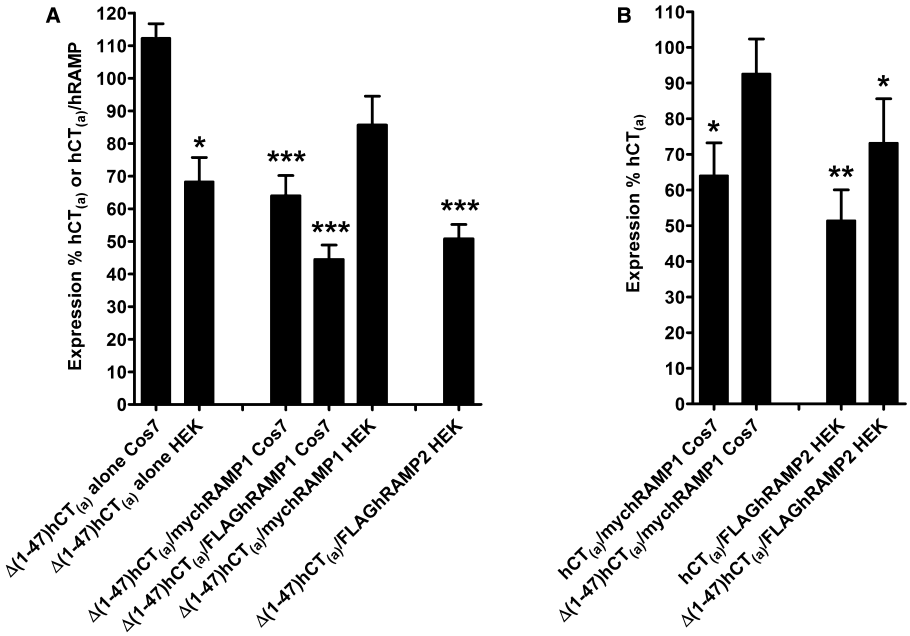

Figure 1

(A) Cell-surface expression of $\Delta(1–47)hCT_{(a)}$ (measuring CTR), $\Delta(1–47)hAMY_{1(a)}$ [$\Delta(1–47)hCT_{(a)}$/mychRAMP1 or $\Delta(1–47)hCT_{(a)}$/FLAGhRAMP1] and $\Delta(1–47)hAMY_{2(a)}$ [$\Delta(1–47)hCT_{(a)}$/FLAGhRAMP2] (measuring the RAMP) in Cos7 and/or in HEK293S cells, shown as a percentage of the relevant control. (B) Cell-surface expression of $hCT_{(a)}$ and $\Delta(1–47)hCT_{(a)}$ in complex with mychRAMP1 in Cos7 cells and FLAGhRAMP2 in HEK293S cells (measuring CTR), shown as a percentage of the relevant control. Data are means ± SEM from three independent experiments, each performed with eight replicates. Data were compared using one-way ANOVA, followed by Dunnett's test using the appropriate control for each data set; $*P < 0.05$; $**P < 0.01$; $***P < 0.001$. For example, the control for '$\Delta(1–47)hCT_{(a)}$ alone HEK' was $hCT_{(a)}$ in HEK cells.

cell-surface expression was also significantly reduced when expressed with Δ(1–47)hCT$_{(a)}$ compared with hCT$_{(a)}$ (Figure 1A). This was not the case in HEK293S cells, where no significant decrease in mychRAMP1 expression was observed (Figure 1A).

In Cos7 cells, we also wanted to confirm that the presence of RAMP1 did not affect Δ(1–47)hCT$_{(a)}$ or hCT$_{(a)}$ expression. In the presence of mychRAMP1, Δ(1–47)hCT$_{(a)}$ expression was higher in complex with RAMP1 compared with hCT$_{(a)}$ expression with RAMP1; however, this was not statistically significant (Figure 1B). Interestingly, hCT$_{(a)}$ expression appeared to be lower in the presence of mychRAMP1 (Figure 1B). Δ(1–47)hCT$_{(a)}$ expression with mychRAMP1 was equivalent to hCT$_{(a)}$ alone. We have interpreted this as RAMP1 partially masking the epitope available for 9B4 antibody binding. Thus, hCT$_{(a)}$/RAMP1 is less able to bind this antibody than hCT$_{(a)}$. In contrast, when the first 47 amino acids of hCT$_{(a)}$ are removed in Δ(1–47)hCT$_{(a)}$, the conformation is such that even when RAMP1 is present, the epitope is available. To confirm that this was related to the antibody used and not a genuine reduction in hCT$_{(a)}$ expression with mychRAMP1, the expression of an HA-tagged version of hCT$_{(a)}$ in the presence and absence of RAMP1 was determined; the data showed that HA-CT$_{(a)}$ expression was not reduced by the presence of RAMP1 (data not shown).

RAMP2 expression was examined only in HEK293S cells. This showed that RAMP2 expression at the cell surface was reduced when expressed with Δ(1–47)hCT$_{(a)}$, compared with hCT$_{(a)}$ (Figure 1A). Similar to RAMP1, hCT$_{(a)}$ expression was apparently lower in the presence of FLAGhRAMP2 (Figure 1B). We tried two tagged versions of RAMP3 (myc or FLAG) but both efficiently translocated to the cell surface in the absence of hCT$_{(a)}$, rendering them unsuitable for this analysis (data not shown). Therefore, we were unable to directly test whether Δ(1–47)hCT$_{(a)}$ affects RAMP3 cell-surface expression.

Receptor pharmacology

The pharmacological profiles for up to six peptide agonists (rAmy, hCT, sCT, hαCGRP, hβCGRP and Tyr°hαCGRP) and two antagonists (sCT$_{8–32}$, AC187) were determined at the different receptors. In most experiments, we measured cAMP, but in some cases, the ability of the peptides to stimulate ERK1/2 phosphorylation was also determined.

hCT$_{(a)}$ and Δ(1–47)hCT$_{(a)}$ pharmacology

In Cos7 cells, there was a significant approximately fivefold reduction in rAmy potency at Δ(1–47)hCT$_{(a)}$ compared with hCT$_{(a)}$ (Figure 2A, Table 1). hCT potency was also significantly reduced at Δ(1–47)hCT$_{(a)}$ compared with hCT$_{(a)}$, displaying an

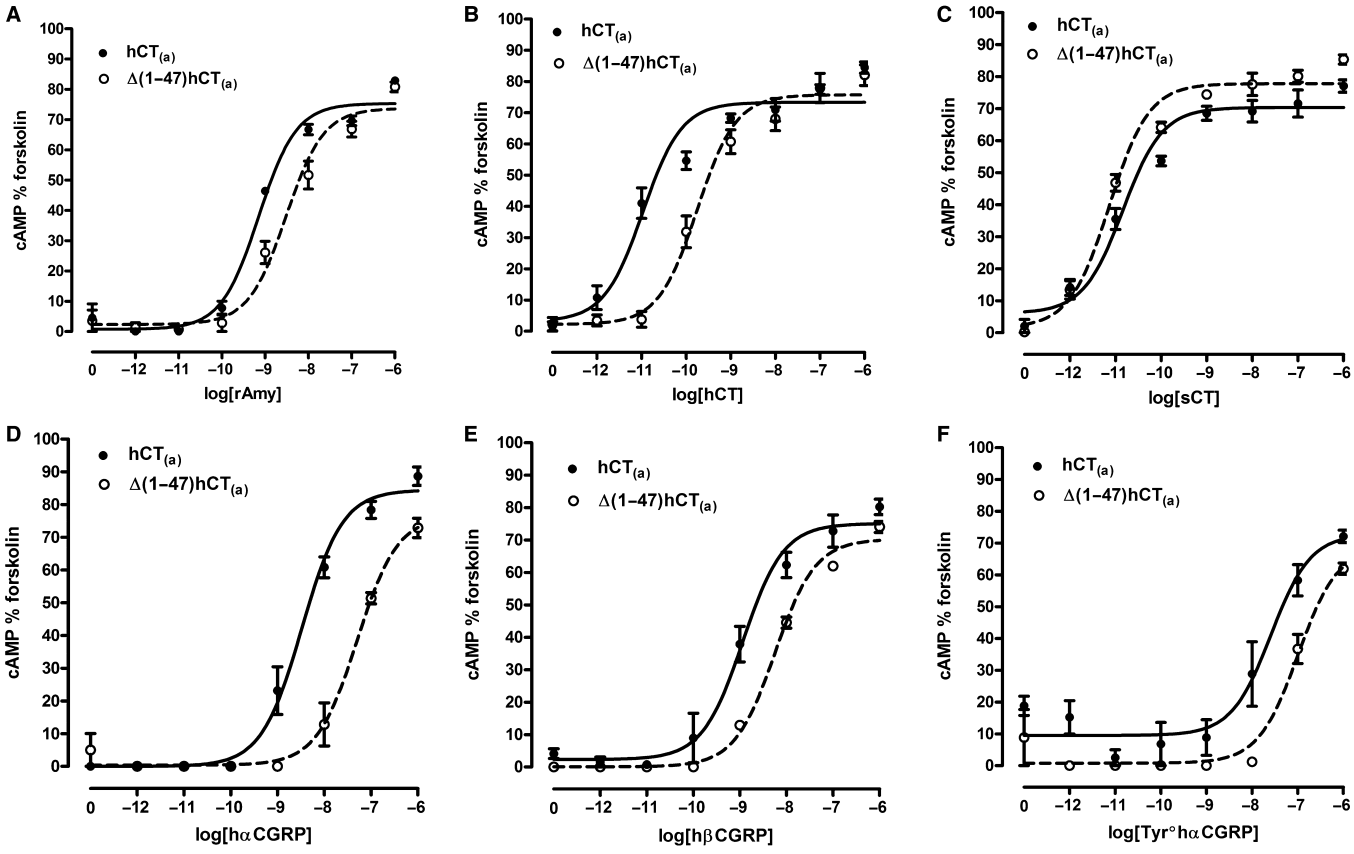

Figure 2

cAMP data for (A) rAmy, (B) hCT, (C) sCT, (D) hαCGRP, (E) hβCGRP and (F) Tyr°hαCGRP responses at hCT$_{(a)}$ and Δ(1–47)hCT$_{(a)}$ in Cos7 cells. The graphs are representatives of three to five independent experiments. Data points are means ± SEM of triplicate assay points.

Table 1

Summary of pEC_{50}'s for cAMP responses in Cos7 cells. *$P < 0.05$; **$P < 0.01$; ***$P < 0.001$ versus full-length receptor control. $^{+}P < 0.05$, $^{++}P < 0.01$, $^{+++}P < 0.001$ versus $hCT_{(a)}$ or $\Delta(1–47)hCT_{(a)}$, as appropriate, by unpaired *t*-tests. Note that the $AMY_{3(a)}$ experiments were conducted at a different time to the $AMY_{1(a)}$ experiments, hence the inclusion of a different set of controls

	$hCT_{(a)}$	$\Delta(1–47)hCT_{(a)}$	$hAMY_{1(a)}$	$\Delta(1–47)hAMY_{1(a)}$
rAmy (n = 4–5)	9.30 ± 0.09	8.63 ± 0.18*	10.5 ± 0.18^{++}	9.98 ± 0.18^{++}
hCT (n = 3–4)	10.7 ± 0.09	9.66 ± 0.21**	10.6 ± 0.35	9.19 ± 0.07**
sCT (n = 5)	10.9 ± 0.24	10.9 ± 0.09	11.1 ± 0.08	10.8 ± 0.20
hαCGRP (n = 3)	8.34 ± 0.09	7.48 ± 0.10**	10.2 ± 0.17^{+++}	10.8 ± 0.09*$^{,+++}$
hβCGRP (n = 3)	9.03 ± 0.11	8.34 ± 0.18*	10.6 ± 0.12	10.4 ± 0.24
Tyr°hαCGRP (n = 3)	7.63 ± 0.13	7.09 ± 0.12*	9.96 ± 0.10	10.1 ± 0.15
	$hCT_{(a)}$	$\Delta(1–47)hCT_{(a)}$	$hAMY_{3(a)}$	$\Delta(1–47)hAMY_{3(a)}$
rAmy (n = 3–5)	8.29 ± 0.07	7.25 ± 0.04***	9.26 ± 0.24^{+}	8.71 ± 0.36^{+}
hCT (n = 3)	10.1 ± 0.18	8.67 ± 0.14**	9.18 ± 0.18^{+}	8.34 ± 0.11*
hαCGRP (n = 3)	7.04 ± 0.21	6.43 ± 0.16	7.91 ± 0.36	8.05 ± 0.32^{++}

Table 2

Summary of pEC_{50}'s for cAMP responses in HEK293S cells. *$P < 0.05$; **$P < 0.01$; ***$P < 0.001$ versus full-length receptor control. $^{+}P < 0.05$; $^{++}P < 0.01$; $^{+++}P < 0.001$ versus $hCT_{(a)}$ or $\Delta(1–47)hCT_{(a)}$, as appropriate, by unpaired *t*-tests

	$hCT_{(a)}$	$\Delta(1–47)hCT_{(a)}$	$hAMY_{1(a)}$	$\Delta(1–47)hAMY_{1(a)}$	$hAMY_{2(a)}$	$\Delta(1–47)hAMY_{2(a)}$
rAmy (n = 3–4)	9.39 ± 0.11	7.84 ± 0.27**	10.1 ± 0.11^{++}	9.53 ± 0.17*$^{,++}$	10.2 ± 0.18^{++}	8.95 ± 0.23**$^{,+}$
hCT (n = 3)	12.0 ± 0.28	10.1 ± 0.25**	–	–	12.1 ± 0.33	9.93 ± 0.14**
hαCGRP (n = 3–6)	8.11 ± 0.03	6.76 ± 0.23***	9.16 ± 0.15^{+++}	9.18 ± 0.15^{+++}	9.17 ± 0.06^{+++}	8.30 ± 0.07***$^{,++}$

~12-fold reduction (Figure 2B, Table 1). On the other hand, $hCT_{(a)}$ and $\Delta(1–47)hCT_{(a)}$ showed equivalent sCT potency (Figure 2C, Table 1). hαCGRP (Figure 2D) and hβCGRP potency (Figure 2E) were both significantly reduced at $\Delta(1–47)hCT_{(a)}$ compared with $hCT_{(a)}$ to a similar magnitude to rAmy (Table 1). Tyr°hαCGRP potency was also significantly reduced at $\Delta(1–47)hCT_{(a)}$ compared with $hCT_{(a)}$, displaying an approximately threefold reduction (Figure 2F, Table 1). There were no differences in E_{max} (data not shown).

$sCT_{8–32}$ is a peptide fragment of sCT and AC187 is a peptide made by replacing the last three residues of $sCT_{8–32}$ with residues 35–37 from rAmy. Both peptides act as antagonists at $AMY_{1(a)}$ and $CT_{(a)}$ receptors (Hay *et al.*, 2005). The potency of $sCT_{8–32}$ was also significantly reduced at $\Delta(1–47)hCT_{(a)}$ compared with $hCT_{(a)}$, displaying an approximately eightfold reduction in pK_B (Table 3, Figure 3A,C). Similar observations were made with AC187 (Table 3, Figure 3B,D).

Three agonists were also tested at the $\Delta(1–47)hCT_{(a)}$ and $hCT_{(a)}$ by cAMP assay in HEK293S cells (Table 2). In a manner similar to our observations in Cos7 cells, hCT, rAmy and hαCGRP potencies were all reduced at $\Delta(1–47)hCT_{(a)}$ compared with $hCT_{(a)}$. The magnitude of this reduction appeared to be greater in HEK293S cells than in Cos7 cells. There were no differences in E_{max} except for a small but significant increase for rAmy at $hCT_{(a)}$ versus $\Delta(1–47)hCT_{(a)}$ (E_{max} ± SEM as % of forskolin-stimulated response; 97.2 ± 1.18 vs. 102 ± 1.44, respectively, $P < 0.05$ by unpaired *t*-test).

Interestingly, when we measured pERK1/2 in Cos 7 cells, there were no differences in hCT or rAmy potency at $\Delta(1–47)hCT_{(a)}$ compared with $hCT_{(a)}$ (Supporting Information Table S2). Agonist potency was generally lower when measuring pERK1/2 rather than cAMP.

$hAMY_{1(a)}$ and $\Delta(1–47)hAMY_{1(a)}$ pharmacology

rAmy responses were first compared between the $hCT_{(a)}$/RAMP1 and $hCT_{(a)}$ to confirm the formation of an $AMY_{1(a)}$ receptor phenotype in Cos7 cells (i.e. a significant enhancement of Amy potency in the presence of RAMP). rAmy was ~15-fold more potent at $hAMY_{1(a)}$ than $hCT_{(a)}$ and ~22-fold more potent at $\Delta(1–47)hAMY_{1(a)}$ than $\Delta(1–47)hCT_{(a)}$ (Table 1). There was a small reduction in rAmy potency at $\Delta(1–47)hAMY_{1(a)}$ compared with $hAMY_{1(a)}$; however, this difference was not statistically significant (Figure 4A).

On the other hand, there was a significant (~25-fold) reduction in hCT potency at $\Delta(1–47)hAMY_{1(a)}$ compared with $hAMY_{1(a)}$ (Figure 4B). hCT responses were also compared between the $AMY_{1(a)}$ and $CT_{(a)}$ receptor phenotypes. hCT was equally potent at both $hAMY_{1(a)}$ and $hCT_{(a)}$ receptors and between $\Delta(1–47)hAMY_{1(a)}$ and $\Delta(1–47)hCT_{(a)}$. sCT potency was comparable between all of these receptors (Figure 4C).

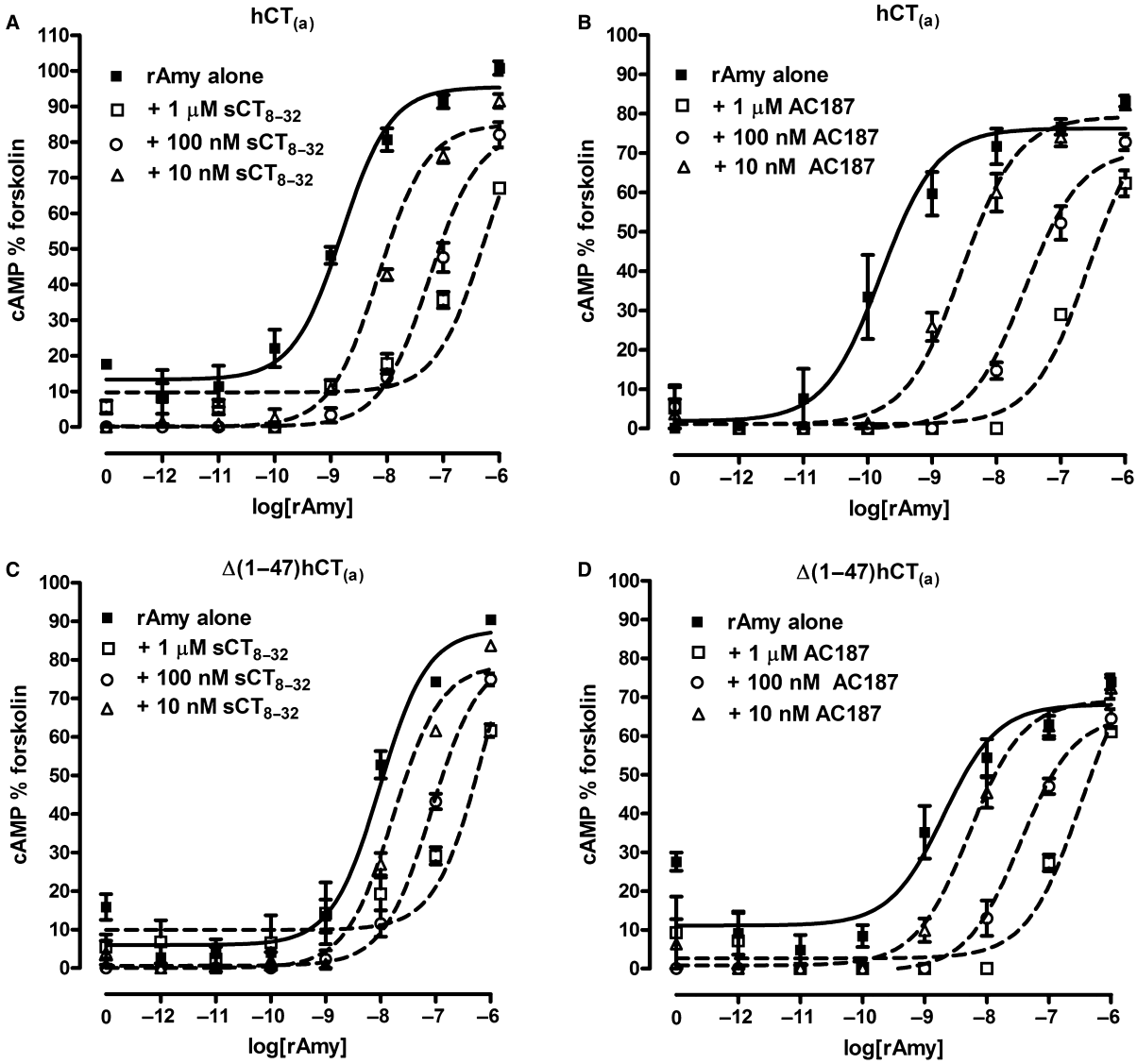

Figure 3

cAMP data for rAmy responses in the presence of three concentrations of sCT_{8-32} or AC187 at (A,B) $hCT_{(a)}$ and (C,D) $\Delta(1-47)hCT_{(a)}$. The graphs are representatives of three to four independent experiments. Data points are means ± SEM of triplicate assay points.

There was a significant approximately fourfold increase in hαCGRP potency at $\Delta(1-47)hAMY_{1(a)}$ compared with $hAMY_{1(a)}$ (Figure 4D). Comparing the $AMY_{1(a)}$ and $CT_{(a)}$ receptor phenotypes, hαCGRP was ~66-fold more potent at $hAMY_{1(a)}$ than $hCT_{(a)}$ and ~1862-fold more potent at $\Delta(1-47)hAMY_{1(a)}$ than $\Delta(1-47)hCT_{(a)}$. hβCGRP was equipotent at both $\Delta(1-47)hAMY_{1(a)}$ and $hAMY_{1(a)}$ (Figure 4E). Comparing the $AMY_{1(a)}$ and $CT_{(a)}$ receptor phenotypes, hβCGRP was ~37-fold more potent at $hAMY_{1(a)}$ than $hCT_{(a)}$ and ~126-fold more potent at $\Delta(1-47)hAMY_{1(a)}$ than $\Delta(1-47)hCT_{(a)}$. Like hβCGRP, Tyr°hαCGRP was equipotent at both $\Delta(1-47)hAMY_{1(a)}$ and $hAMY_{1(a)}$ (Figure 4F). The Tyr°hαCGRP responses were also compared between the $AMY_{1(a)}$ with $CT_{(a)}$ receptor phenotypes. Tyr°hαCGRP was ~214-fold more potent at $hAMY_{1(a)}$ than $hCT_{(a)}$ and ~1047-fold more potent at $\Delta(1-47)hAMY_{1(a)}$ than $\Delta(1-47)hCT_{(a)}$.

The E_{max} was not significantly different in any of the comparisons above except for a small but significant reduction in the maximum response for sCT at $\Delta(1-47)hAMY_{1(a)}$ compared with $\Delta(1-47)hCT_{(a)}$ (E_{max} ± SEM; 69.3 ± 1.92 vs. 75.8 ± 0.99, respectively, $P < 0.05$ by unpaired *t*-test).

The $\Delta(1-47)hCT_{(a)}$ and $\Delta(1-47)hAMY_{1(a)}$ receptors were also characterized with antagonists sCT_{8-32} (Figure 5A,C) and AC187 (Figure 5B,D), using rAmy as the agonist (Table 3). There was a small reduction in pK_B for sCT_{8-32} at $\Delta(1-47)hAMY_{1(a)}$ compared with $hAMY_{1(a)}$; however, it was not statistically significant. sCT_{8-32} potency was compared between the $AMY_{1(a)}$ and $CT_{(a)}$ receptor phenotypes. sCT_{8-32} was approximately sevenfold less potent an antagonist of $hAMY_{1(a)}$ compared with $hCT_{(a)}$. The pK_B for sCT_{8-32} was also slightly lower at $\Delta(1-47)hAMY_{1(a)}$ compared with $\Delta(1-47)hCT_{(a)}$; however, the reduction was not statistically significant.

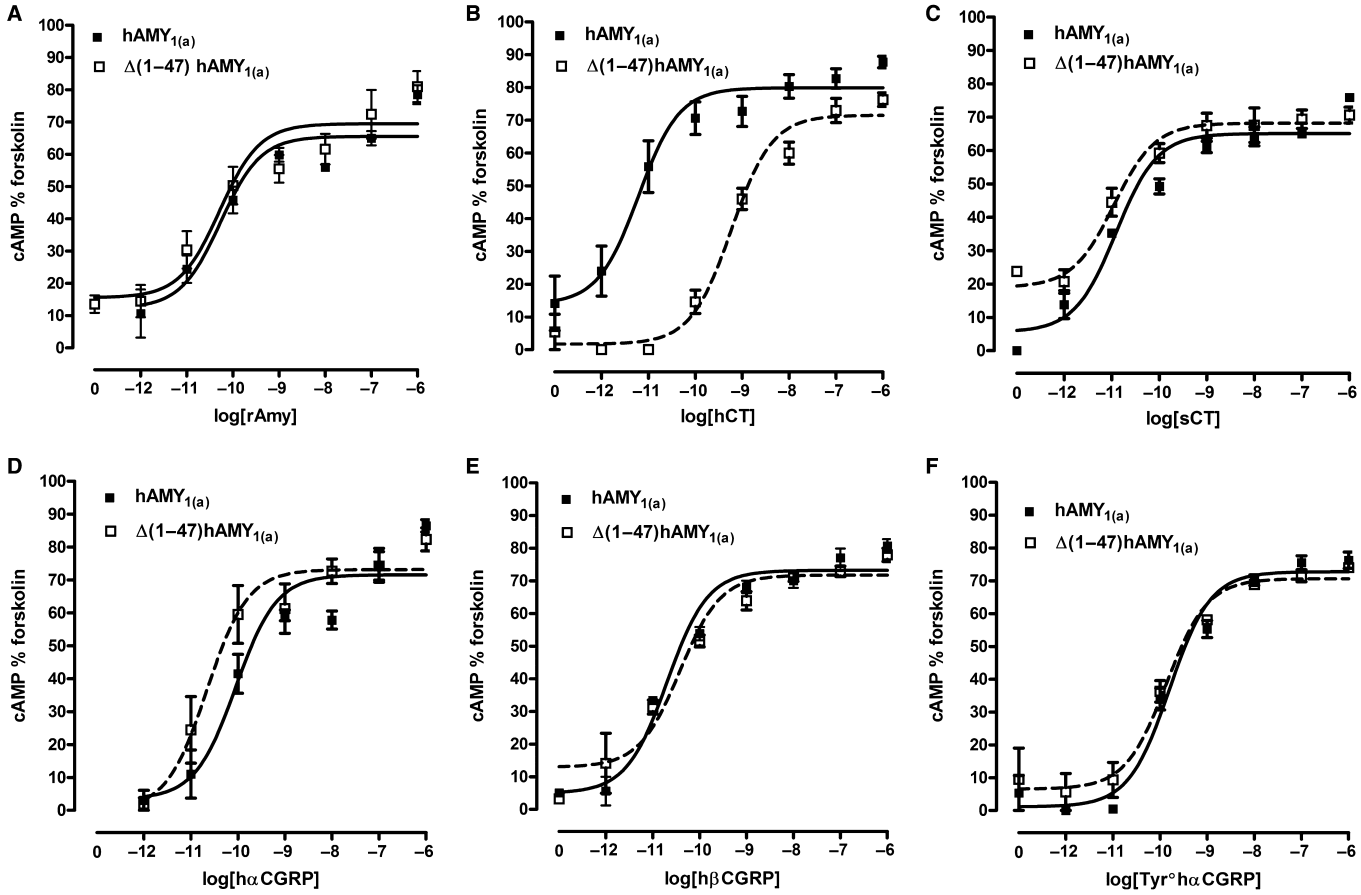

Figure 4

cAMP data for (A) rAmy, (B) hCT, (C) sCT, (D) hαCGRP, (E) hβCGRP and (F) Tyr°hαCGRP responses at $hAMY_{1(a)}$, $\Delta(1–47)hAMY_{1(a)}$ in Cos7 cells. The graphs are representatives of three to five independent experiments. Data points are means ± SEM of triplicate assay points.

Table 3

pK_B values for $sCT_{8–32}$ and AC187 in antagonizing rAmy responses at $hAMY_{1(a)}$, $\Delta(1–47)hAMY_{1(a)}$, $hCT_{(a)}$ and $\Delta(1–47)hCT_{(a)}$ measured in cAMP assay in Cos7 cells. $^{**}P < 0.01$ versus full-length receptor control. $^{+}P < 0.05$ versus $hCT_{(a)}$ or $\Delta(1–47)hCT_{(a)}$, as appropriate, by unpaired *t*-tests

	$hCT_{(a)}$	$\Delta(1–47)\ hCT_{(a)}$	$hAMY_{1(a)}$	$\Delta(1–47)\ hAMY_{1(a)}$
$sCT_{8–32}$ (n = 3–4)	8.95 ± 0.17	8.03 ± 0.12**	8.08 ± 0.28^{+}	7.57 ± 0.31
AC187 (n = 4)	8.85 ± 0.16	7.82 ± 0.16**	9.25 ± 0.07	8.43 ± 0.14$^{**,+}$

AC187 also produced rightward shifts in the concentration–response curve for rAmy with no suppression of maximum response at all receptors. There was a significant approximately sevenfold reduction in pK_B for AC187 at $\Delta(1–47)hAMY_{1(a)}$ compared with $hAMY_{1(a)}$. The pK_B for AC187 was slightly higher at $hAMY_{1(a)}$ compared with $hCT_{(a)}$; however, this was not statistically significant. This small difference (approximately threefold) did reach statistical significance at $\Delta(1–47)hAMY_{1(a)}$ receptor compared with $\Delta(1–47)hCT_{(a)}$.

cAMP assay in HEK293S cells also revealed a decrease in rAmy potency at $\Delta(1–47)hAMY_{1(a)}$ compared with $hAMY_{1(a)}$, which was statistically significant (Table 2). There was no difference in hαCGRP potency between these receptors in these cells. Due to the low potency of rAmy at $\Delta(1–47)hCT_{(a)}$, the magnitude of enhancement of rAmy potency at $\Delta(1–47)hCT_{(a)}$ compared with $\Delta(1–47)hAMY_{1(a)}$ was much greater (~50-fold) compared with the full-length receptors (~5-fold). This was also the case for enhancement of hαCGRP potency between these receptors (~250-fold vs. ~10 fold). E_{max} was reduced at $\Delta(1–47)hCT_{(a)}$ in the presence of RAMP1 for these two agonists (rAmy: E_{max} ± SEM; 102 ± 1.44 for $\Delta(1–47)hCT_{(a)}$; 86.7 ± 2.67 for $\Delta(1–47)hAMY_{1(a)}$; $P < 0.01$ by unpaired t-test. hαCGRP: E_{max} ± SEM; 103 ± 5.68 for $\Delta(1–47)hCT_{(a)}$; 75.1 ± 8.46 for $\Delta(1–47)hAMY_{1(a)}$; $P < 0.05$ by unpaired *t*-test).

When we measured pERK1/2 in Cos7 cells, there was no significant enhancement in rAmy potency with either Δ(1–

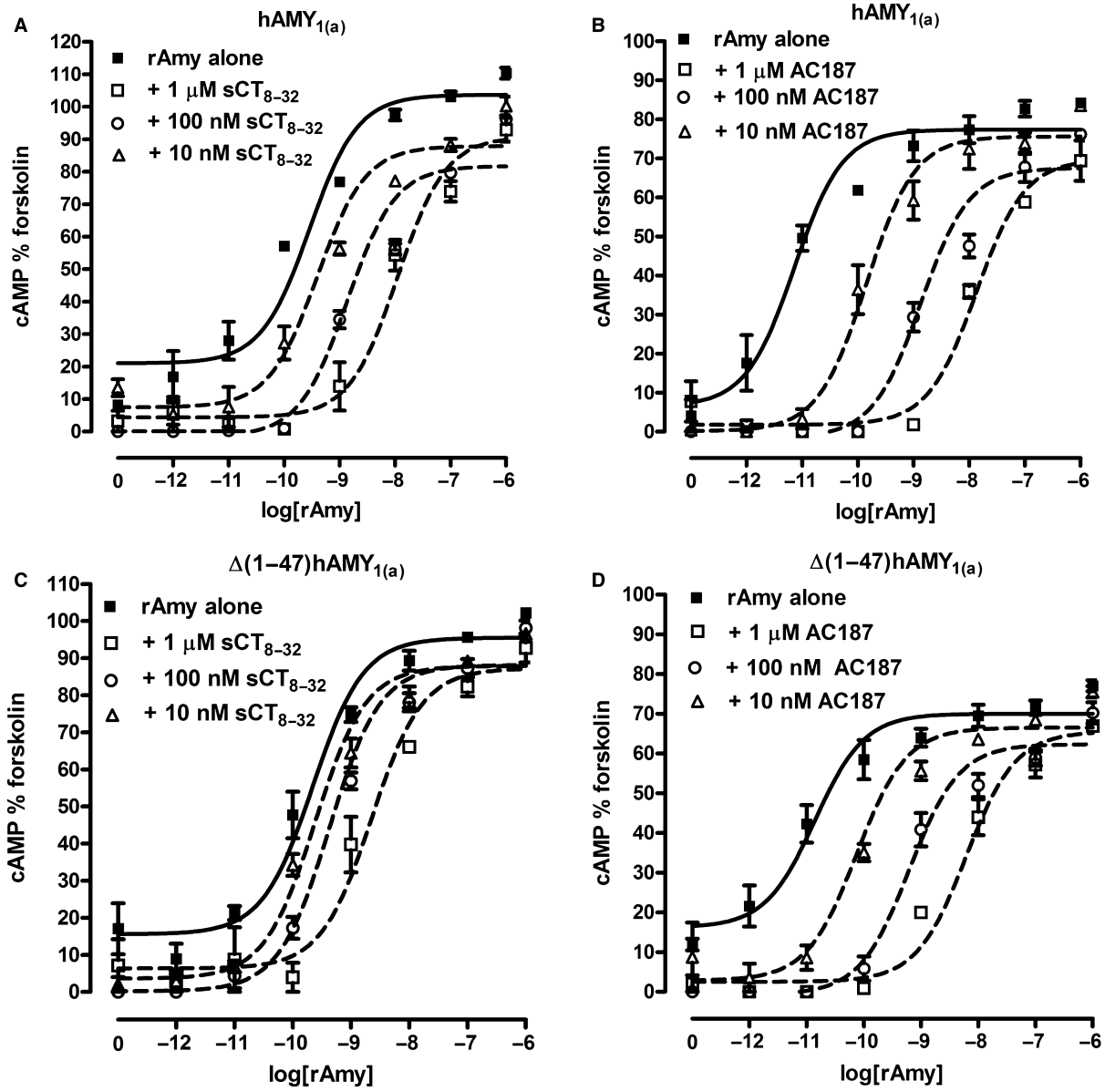

Figure 5

cAMP data for rAmy responses in the presence of three concentrations of sCT_{8-32} or AC187 at (A,B) $hAMY_{1(a)}$ and (C,D) $\Delta(1–47)hAMY_{1(a)}$. The graphs are representatives of three to four independent experiments. Data points are means ± SEM of triplicate assay points.

47)$hCT_{(a)}$ or $hCT_{(a)}$ in the presence of RAMP1 (Supporting Information Table S2). Therefore, there was no significant induction of AMY receptor phenotype when pERK1/2 was measured. hCT potency was also unchanged.

$hAMY_{2(a)}$ and $\Delta(1–47)hAMY_{2(a)}$ pharmacology

Pharmacological characterization of these receptors was only performed in HEK293S cells because only weak AMY phenotype is generated with RAMP2 in Cos7 cells (Table 2, Figure 6). rAmy and hαCGRP potency was enhanced in the presence of RAMP2 at both receptors, whereas hCT potency did not change. However, the potency of all agonists (hCT, rAmy and hαCGRP) was substantially reduced at Δ(1–47)$hAMY_{2(a)}$ compared with $hAMY_{2(a)}$. The E_{max} was not significantly different in any of the comparisons except for a reduction in the maximum response for hαCGRP at Δ(1–47)$hAMY_{2(a)}$ compared with $hAMY_{2(a)}$ (E_{max} ± SEM; 88.7 ± 0.32 vs. 94.8 ± 0.81, respectively, $P < 0.01$ by unpaired *t*-test).

$hAMY_{3(a)}$ and $\Delta(1–47)hAMY_{3(a)}$ pharmacology

These experiments were conducted in Cos7 cells. With RAMP3, the only agonist to differ between $hAMY_{3(a)}$ and Δ(1–47)$hAMY_{3(a)}$ was hCT (Figure 7B). rAmy (Figure 7A) and hαCGRP (Figure 7C) potency did not significantly differ between receptors, although there was a trend to a decrease in rAmy potency (Table 1). The formation of $hAMY_{3(a)}$ receptor

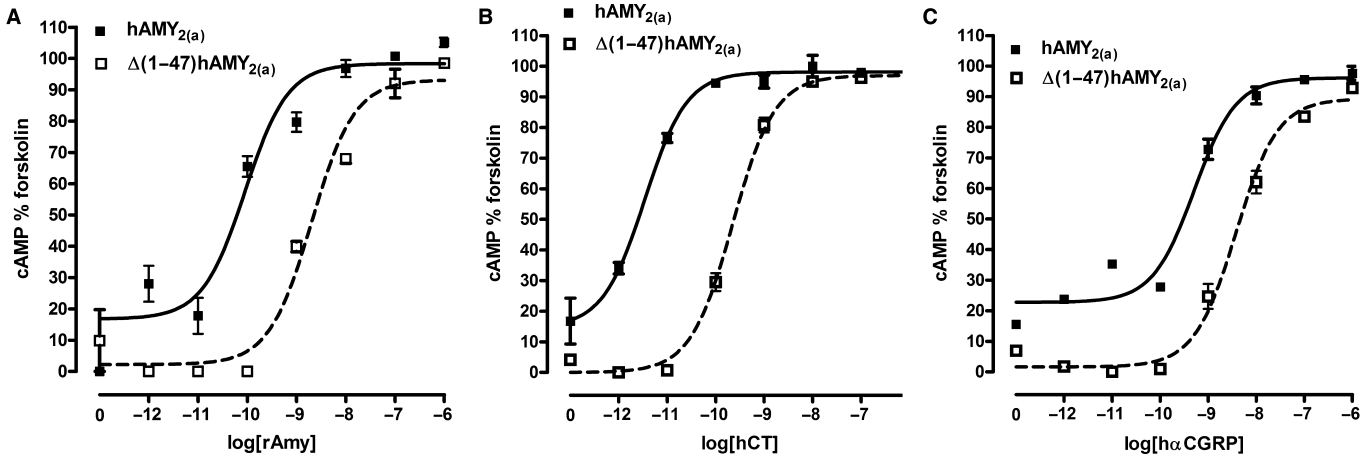

Figure 6

cAMP data for (A) rAmy, (B) hCT, (C) hαCGRP responses at $hAMY_{2(a)}$, $\Delta(1–47)hAMY_{2(a)}$ in HEK293S cells. The graphs are representative of three to four independent experiments. Data points are means ± SEM of triplicate assay points.

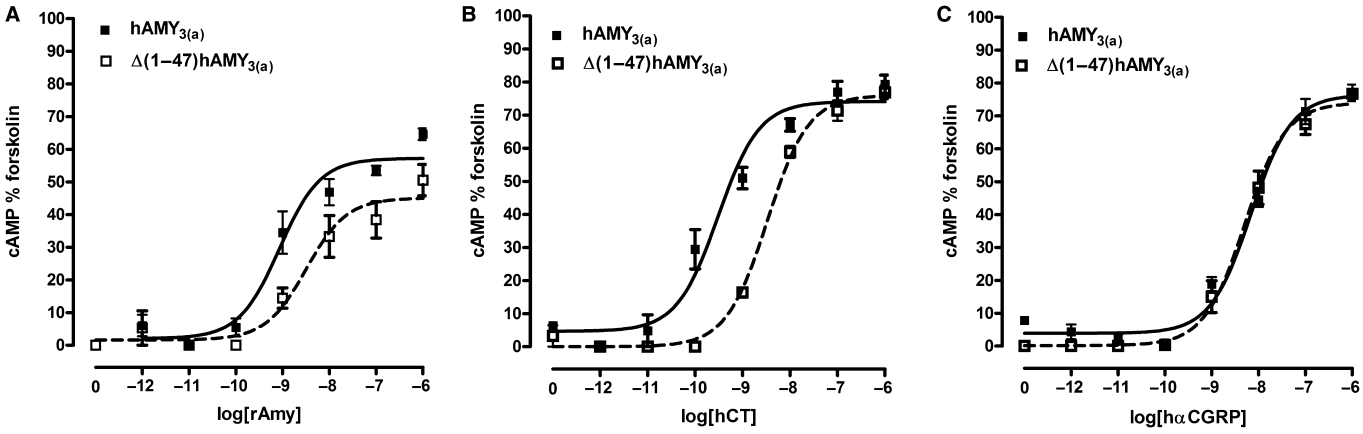

Figure 7

cAMP data for (A) rAmy, (B) hCT, (C) hαCGRP responses at $hAMY_{3(a)}$, $\Delta(1–47)hAMY_{3(a)}$ in Cos7 cells. The graphs are representative of three to five independent experiments. Data points are means ± SEM of triplicate assay points.

phenotype was also analysed in Cos7 cells. rAmy was ~9-fold more potent at $hAMY_{3(a)}$ than $hCT_{(a)}$ and ~29-fold more potent at $\Delta(1–47)hAMY_{3(a)}$ than $\Delta(1–47)hCT_{(a)}$ (Table 1). In contrast, there was approximately sevenfold reduction in hCT potency at $hAMY_{3(a)}$ compared with $hCT_{(a)}$, while a non-significant approximately twofold reduction was observed in hCT potency at $\Delta(1–47)hAMY_{3(a)}$ compared with $\Delta(1–47)hCT_{(a)}$. hαCGRP was approximately sevenfold more potent at $hAMY_{3(a)}$ than $hCT_{(a)}$, but statistical significance was not achieved. On the other hand, there was an ~42-fold increase in hαCGRP potency at $\Delta(1–47)hAMY_{3(a)}$ compared with $\Delta(1–47)hCT_{(a)}$. There were no significant differences in E_{max} (data not shown).

The contribution of the I347T mutation to $\Delta(1–47)hCT_{(a)}$ phenotype

An isoleucine to threonine point mutation was identified at position 347 in the sequence of the truncated $hCT_{(a)}$ variant cloned by Albrandt *et al.* (1995). In order to determine the contribution of this substitution to the variant phenotype, we made $\Delta(1–47)hCT_{(a)}$-I347. This construct has the identical amino acid sequence as $\Delta(1–47)hCT_{(a)}$, except that it has an isoleucine residue at position 347 instead of threonine. Cell-surface expression of $\Delta(1–47)hCT_{(a)}$-I347 both in the presence and absence of RAMP1 was determined, and rAmy, hCT and hαCGRP responses were compared (Table 4).

$\Delta(1–47)hCT_{(a)}$-I347 expression was enhanced by 58% compared with $\Delta(1–47)hCT_{(a)}$, but no significant difference was observed when they were co-expressed with RAMP1. RAMP1 expression in these complexes were also studied; the expressions of $\Delta(1–47)AMY_{1(a)}$ and $\Delta(1–47)AMY_{1(a)}$-I347 were not significantly different from each other.

The functional analysis of the receptors showed that there was no significant difference in rAmy, hCT or hαCGRP potency between $\Delta(1–47)AMY_{1(a)}$-I347 versus $\Delta(1–47)AMY_{1(a)}$ and $\Delta(1–47)hCT_{(a)}$-I347 versus $\Delta(1–47)hCT_{(a)}$ (Table 4).

Table 4

Summary of pEC_{50} for peptide responses at Δ(1–47) $hAMY_{1(a)}$, Δ(1–47) $hAMY_{1(a)}$-I347, Δ(1–47)$hCT_{(a)}$ and Δ(1–47) $hCT_{(a)}$-I347 measured in cAMP assays and their cell-surface expression levels in Cos7 cells. Data were analysed using unpaired *t*-test for cAMP assays and one-way ANOVA, followed by Tukey's test for ELISAs. $^{**}P < 0.01$ and $^{***}P < 0.001$ compared with the WT receptors; $^{+}P < 0.05$ compared with Δ(1–47)$hCT_{(a)}$ or Δ(1–47) $hAMY_{1(a)}$

	pEC_{50} (n = 3)			Cell-surface expression (n = 3)	
Receptor	rAmy	hCT	hαCGRP	mychRAMP1 expression (% $hAMY_{1(a)}$ expression)	$hCT_{(a)}$ expression (% $hCT_{(a)}$ alone expression)
Δ(1–47)$hAMY_{1(a)}$	8.98 ± 0.29	8.25 ± 0.11	9.08 ± 0.26	64.0 ± 6.24***	92.6 ± 9.74
Δ(1–47)$hAMY_{1(a)}$-I347	9.08 ± 0.19	8.15 ± 0.09	9.15 ± 0.22	77.2 ± 4.00**	123 ± 12.4
Δ(1–47)$hCT_{(a)}$	7.25 ± 0.04	8.67 ± 0.14	6.43 ± 0.16	–	112 ± 4.39
Δ(1–47)$hCT_{(a)}$-I347	7.33 ± 0.27	8.06 ± 0.14	6.25 ± 0.12	–	177 ± 25.5**,+

Therefore, the I347T substitution seems to make little contribution to Δ(1–47)$hCT_{(a)}$ phenotype.

Discussion

Signal peptides have been suggested to play a crucial role in the expression of family B GPCRs (Couvineau *et al.*, 2004). However, removal of the first 47 residues in the N terminus, including the predicted signal peptide, did not substantially impact upon the cell-surface expression of Δ(1–47)$hCT_{(a)}$. In Cos7 cells, expression of Δ(1–47)$hCT_{(a)}$ was slightly higher than $hCT_{(a)}$, while in HEK293S cells, a modest reduction of ~30% in expression was observed. It has previously been reported that the same CTR/RAMP complexes exhibit different signalling profiles in different cellular backgrounds, likely due to the expressed complement of proteins that is unique to each cell type (Morfis *et al.*, 2008). Therefore, the difference in expression may be related to the differential cellular backgrounds between Cos7 and HEK293 cells. On this basis, the predicted signal peptide does not appear to play a major role in CTR.

Δ(1–47)$hCT_{(a)}$ gives the first insight into the mode of RAMP interaction with CTR. In Cos7 cells, there was a reduction in both mychRAMP1 and FLAGhRAMP1 translocation to the cell surface with Δ(1–47)$hCT_{(a)}$, compared with the full-length receptor, but this effect was much smaller (~10% reduction) and was not statistically significant in HEK293S cells. Again, this difference observed in Cos7 versus HEK293 cells may reflect the individual properties of the two cell types. Therefore, it seems unlikely that the first 47 amino acids of CTR play a major role in associating with RAMP1. A previous study using mouse CLR and human PTH (parathyroid hormone) receptor chimeras showed that N terminal residues 23–60 of the closely related CLR were important for mouse CLR and mouse RAMP1 association (Ittner *et al.*, 2005). The crystal structure of the extracellular domains of the human CLR/RAMP1 complex shows that the major interactions involve residues on the αC1 helix of hCLR spanning methionine 42 to glutamine 54 (Haar *et al.*, 2010). Amino acid sequence alignment shows that methionine 42 of CLR corresponds to methionine 49 of hCTR, which is beyond the truncated region in Δ(1–47)$hCT_{(a)}$. Although there is no structure available for the extracellular domain of CTR, it is likely that CTR and CLR adopt a similar structure and that methionine 49 and beyond in CTR may be principally responsible for RAMP1 interactions in the $AMY_{1(a)}$ receptor.

Our data suggest that CTR may interact differently with RAMP2. While RAMP1 expression was unaffected with Δ(1–47)$hCT_{(a)}$ in HEK293S cells, RAMP2 translocation to the cell surface was reduced by approximately 50%. Residues 1–47 of CTR may be more important for RAMP2 than RAMP1 association. The recent publication of the crystal structure of the extracellular domains of the CLR/RAMP2 complex showed several differences between CLR/RAMP1 and CLR/RAMP2 complexes (Haar *et al.*, 2010; Kusano *et al.*, 2012). In particular, CLR/RAMP interfaces were suggested to be different between the two complexes, where RAMP2 is distinctly orientated from CLR compared with RAMP1. It is thus likely that differences in the protein to protein interface may also be expected in the CTR/RAMP complexes; some residues in regions 1–47 may be more critical to CTR/RAMP2 association compared with those in CTR/RAMP1 complexes. We were unable to compare effects with RAMP3 due to tag artefacts.

hCT potency was significantly reduced at Δ(1–47)$hCT_{(a)}$ compared with $hCT_{(a)}$ in both cell types, suggesting that the first 47 amino acids of the receptor contain a region or residue important for hCT interactions. This is consistent with a previous investigation where a photoaffinity hCT probe labelled residue T30 in the N terminus of $hCT_{(a)}$ (Dong *et al.*, 2004a). The exact contribution of T30 of $hCT_{(a)}$ to its interaction with hCT is not clear; alanine substitution at this position showed normal binding and cAMP response to hCT, but a nearby residue may be important (Dong *et al.*, 2004b). The potency of all other peptides, apart from sCT, was also reduced at Δ(1–47)$hCT_{(a)}$ compared with $hCT_{(a)}$ in both cell types. It is possible that this was due to a reduction in cell-surface expression in HEK293S cells. However, cell-surface expression was not reduced in Cos7 cells, suggesting that it is more likely that there may be one or more interaction sites within the first 47 amino acids of $hCT_{(a)}$ that are important for interactions with these peptides, or the truncation altered the receptor conformation, which, in turn, affected the peptide interactions. Both $hCT_{(a)}$ and Δ(1–47)$hCT_{(a)}$ displayed

a potency order of sCT > hCT > rAmy > CGRP (Supporting Information Table S3). This is consistent with the initial characterization performed where both the full-length and the truncated $hCT_{(a)}$ showed a potency order of sCT > hCT > hAmy (Albrandt *et al.*, 1995). In the previous study, Amy potency seemed to be reduced at $\Delta(1–47)hCT_{(a)}$, which was consistent with our work. Unchanged sCT potency is also consistent between studies. On the other hand, we see a clear reduction in hCT potency in two cell backgrounds. Formerly, there was no reduction in hCT potency. Given that both studies have used Cos7 cells, the reason for this discrepancy is unclear.

sCT displayed high and equivalent potency at the truncated and full-length $hCT_{(a)}$. To further investigate this, we used two other sCT derivatives, $sCT_{8–32}$, a peptide fragment of sCT, and AC187, a peptide made by replacing the last three amino acids of $sCT_{8–32}$ with those from rAmy. Both peptides serve as antagonists at $CT_{(a)}$ and $AMY_{1(a)}$ receptors (Hay *et al.*, 2005). Both peptides had lower affinity at $\Delta(1–47)hCT_{(a)}$ compared with the full-length $hCT_{(a)}$ receptor. This apparently contradicts the full-length sCT data but sCT is a very potent/high affinity agonist that elicits poor reversibility of binding to human CTR; on the other hand, antagonists including $CT_{8–32}$ bind reversibly to the receptor (Hilton *et al.*, 2000; Poyner *et al.*, 2002). Therefore, an effect of the CTR truncation may be difficult to detect for full-length sCT.

The differential peptide responses seen at the different AMY receptors versus $hCT_{(a)}$ were consistent with the previously published data (Hay *et al.*, 2005). For example, rAmy, CGRP and hCT were approximately equipotent at $hAMY_{1(a)}$, while hCT was more potent than rAmy or CGRP at $hCT_{(a)}$. The formation of AMY receptor phenotype by $\Delta(1–47)hCT_{(a)}$ was evident for all three RAMPs, despite variable reductions in RAMP1 or RAMP2 translocation to the cell surface. Peptide potencies for rAmy, hαCGRP, hβCGRP and Tyr°hαCGRP were all enhanced at $\Delta(1–47)hAMY_{1(a)}$ compared with $\Delta(1–47)hCT_{(a)}$, indicating that $\Delta(1–47)hCT_{(a)}$ still associates with RAMP1 and forms a functional $hAMY_{1(a)}$ receptor. In addition, $\Delta(1–47)hAMY_{1(a)}$ appeared to be fully functional at the cell surface, displaying equivalent peptide responses to the full-length receptor for all agonists tested except for hCT. In particular, $\Delta(1–47)hAMY_{1(a)}$ exhibited a potent CGRP receptor phenotype, displaying a higher potency towards hαCGRP than rAmy. This potency was even greater than that elicited from full-length $hAMY_{1(a)}$ receptor and demonstrated altered peptide potency order (Supporting Information Table S3). Like RAMP1, the AMY receptor phenotype was observed for $\Delta(1–47)hAMY_{2(a)}$ as peptide potencies of rAmy and hαCGRP were significantly enhanced in the presence of RAMP2. $\Delta(1–47)hAMY_{3(a)}$ also displayed an AMY receptor pharmacology where both rAmy and hαCGRP potencies were significantly enhanced in the presence of RAMP3.

The phenotype of $\Delta(1–47)hCT_{(a)}$ in the presence of RAMPs was particularly interesting. hαCGRP, hβCGRP and Tyr°hαCGRP potencies, which were reduced at $\Delta(1–47)hCT_{(a)}$, were restored at $\Delta(1–47)hAMY_{1(a)}$; all these agonists showed equivalent or even higher peptide potencies at $\Delta(1–47)hAMY_{1(a)}$ compared with $hAMY_{1(a)}$. This effect was particularly clear for hαCGRP, which showed no loss of activity at $\Delta(1–47)hCT_{(a)}$ in the presence of RAMP1 in Cos7 or HEK293S cells. It seems that the presence of RAMP1 essentially rescued the function of this receptor, with respect to CGRP and generated a receptor with a unique pharmacological profile. RAMP3 had a similar effect to RAMP1, where hαCGRP potency was also maintained at $\Delta(1–47)hAMY_{3(a)}$ compared with $hAMY_{3(a)}$. Therefore, RAMP1 and RAMP3 may have a role in stabilizing some peptide interactions sites in the $\Delta(1–47)hCT_{(a)}$ receptor, either by directly contributing peptide contacts or altering the receptor conformation. On the other hand, RAMP2 did not appear to play such a role in rescuing CGRP potency at $\Delta(1–47)hAMY_{2(a)}$; hαCGRP potency was also reduced at $\Delta(1–47)hAMY_{2(a)}$ compared with $hAMY_{2(a)}$. This is consistent with the pharmacology of receptor complexes, where RAMPs 1 and 3 tend to support higher affinity CGRP interactions than RAMP2 (Poyner *et al.*, 2002; Gingell *et al.*, 2010; Moore *et al.*, 2010). rAmy potency was affected most in RAMP2 complexes. The overall magnitude of reduction in potency observed at the truncated receptors was greater for $hAMY_{2(a)}$ receptors compared with $hAMY_{1(a)}$ receptors. It is possible that these effects were related to reduction in expression of with $\Delta(1–47)hAMY_{2(a)}$ at the cell surface.

Despite the changes seen in cAMP accumulation between $\Delta(1–47)hCT_{(a)}$/$\Delta(1–47)hAMY_{1(a)}$ and full-length receptors, no differences in ERK1/2 phosphorylation were observed. The reason for this is not yet defined because the mechanisms for ERK regulation at these receptors are not well defined. This could reflect distinct receptor conformations with the removal of residues 1–47 disturbing the conformation, leading to cAMP accumulation but not that needed for ERK1/2 phosphorylation. It could also reflect non-stoichiometric regulation of ERK, such that a submaximal cAMP response is still compatible with maximal ERK1/2 phosphorylation. Each receptor splice variant, coupled with individual RAMPs, creates essentially new receptor units, each with potentially unique properties in terms of ligand interaction and signalling characteristics. More work is needed to determine the relevance of ERK1/2 phosphorylation versus cAMP to CT and Amy biology and in particular what the predominant signalling mechanism might be for $\Delta(1–47)hCT_{(a)}$ expressed in native tissues. A cell-type heavily reliant on cAMP for CT function might be more affected by this receptor variant than one in which ERK1/2 is more significant.

The effect of the I347T mutation found in $\Delta(1–47)hCT_{(a)}$ was also determined in this study. There was little effect in receptor expression with this mutation apart from an enhanced $\Delta(1–47)hCT_{(a)}$ expression when isoleucine was present at position 347. Furthermore, $\Delta(1–47)hCT_{(a)}$ receptor function was not affected both in the presence and in the absence of RAMP1. Therefore, the I347T mutation reported in the previous study (Albrandt *et al.*, 1995) does not seem to have any major impact to $(\Delta(1–47)hCT_{(a)}$ receptor expression or function. I347T could be a sequencing artefact.

In this study, a naturally occurring variant of $hCT_{(a)}$ containing a 1–47 truncation at the N terminus has been characterized. Despite lacking the first 47 amino acids in the N terminus, $\Delta(1–47)hCT_{(a)}$ retains its ability to reach the cell surface. RAMP association is mostly retained and the $\Delta(1–47)AMY_{1(a)}$ receptor is a super-potent CGRP receptor. On the other hand, $\Delta(1–47)hCT_{(a)}$ loses functionality as a CT receptor, suggesting that residues 1–47 may either have a role in maintaining overall receptor structure or possibly contain

one or more interaction sites for peptides. Thus, the functionality of the $\Delta(1–47)hCT_{(a)}$ variant depends on whether it is co-expressed with RAMP and with which RAMP it is expressed. $\Delta(1–47)hCT_{(a)}$ expression has been detected by Southern blot in a range of human tissues, including kidney, skeletal muscle, lung and hypothalamus (Albrandt *et al.*, 1995). In kidney, this could potentially result in reduced CT responsiveness (Findlay and Sexton, 2004). On the other hand, CGRP responsiveness could be enhanced if RAMP1 were co-expressed with this variant. Unfortunately, there is no corresponding information on RAMP expression or Amy/CGRP function in these human tissues and so it is very difficult to speculate as to the physiological function of this variant. Nevertheless, the data presented here certainly indicate that where RAMPs are co-expressed with this CTR splice variant, the resulting receptors could contribute to the actions of Amy and CGRP. The potential contributions of such receptors to the physiology of these peptides should not be overlooked, although teasing out their individual roles will be a challenging task.

Acknowledgements

The Health Research Council (NZ) is thanked for their support (to D. L. H.). Portions of this work were also partially supported by the National Institutes of Health grant DK46577 (to L. J. M.). We thank Peter Wookey for providing the 9B4 antibody.

Conflict of interest

None for any author.

References

Albrandt K, Brady EM, Moore CX, Mull E, Sierzega ME, Beaumont K (1995). Molecular cloning and functional expression of a third isoform of the human calcitonin receptor and partial characterization of the calcitonin receptor gene. Endocrinology 136: 5377–5384.

Bailey RJ, Hay DL (2006). Pharmacology of the human CGRP1 receptor in Cos 7 cells. Peptides 27: 1367–1375.

Bailey RJ, Hay DL (2007). Agonist-dependent consequences of proline to alanine substitution in the transmembrane helices of the calcitonin receptor. Br J Pharmacol 151: 678–687.

Christopoulos G, Perry KJ, Morfis M, Tilakaratne N, Gao Y, Fraser NJ *et al.* (1999). Multiple amylin receptors arise from receptor activity-modifying protein interaction with the calcitonin receptor gene product. Mol Pharmacol 56: 235–242.

Cooper GJ, Willis AC, Clark A, Turner RC, Sim RB, Reid KB (1987). Purification and characterization of a peptide from amyloid-rich pancreases of type 2 diabetic patients. Proc Natl Acad Sci U S A 84: 8628–8632.

Couvineau A, Rouyer-Fessard C, Laburthe M (2004). Presence of a N-terminal signal peptide in class II G protein-coupled receptors: crucial role for expression of the human VPAC1 receptor. Regul Pept 123: 181–185.

Dong M, Pinon DI, Cox RF, Miller LJ (2004a). Importance of the amino terminus in secretin family G protein-coupled receptors. Intrinsic photoaffinity labeling establishes initial docking constraints for the calcitonin receptor. J Biol Chem 279: 1167–1175.

Dong M, Pinon DI, Cox RF, Miller LJ (2004b). Molecular approximation between a residue in the amino-terminal region of calcitonin and the third extracellular loop of the class B G protein-coupled calcitonin receptor. J Biol Chem 279: 31177–31182.

Findlay DM, Sexton PM (2004). Calcitonin. Growth Factors 22: 217–224.

Fineman M, Weyer C, Maggs DG, Strobel S, Kolterman OG (2002). The human amylin analog, pramlintide, reduces postprandial hyperglucagonemia in patients with type 2 diabetes mellitus. Horm Metab Res 34: 504–508.

Furness SGB, Wootten D, Christopoulos A, Sexton PM (2012). Consequences of splice variation on Secretin family G protein-coupled receptor function. Br J Pharmacol 166: 98–109.

Gingell JJ, Qi T, Bailey RJ, Hay DL (2010). A key role for tryptophan 84 in receptor activity-modifying protein 1 in the amylin 1 receptor. Peptides 31: 1400–1404.

Guidobono F, Coluzzi M, Pagani F, Pecile A, Netti C (1994). Amylin given by central and peripheral routes inhibits acid gastric secretion. Peptides 15: 699–702.

ter Haar E, Koth CM, Abdul-Manan N, Swenson L, Coll JT, Lippke JA *et al.* (2010). Crystal structure of the ectodomain complex of the CGRP receptor, a class-B GPCR, reveals the site of drug antagonism. Structure 18: 1083–1093.

Hay DL, Christopoulos G, Christopoulos A, Poyner DR, Sexton PM (2005). Pharmacological discrimination of calcitonin receptor-receptor activity modifying protein complexes. Mol Pharmacol 67: 1655–1665.

Hay DL, Christopoulos G, Christopoulos A, Sexton PM (2006). Determinants of 1-piperidinecarboxamide, N-[2-[[5-amino-l-[[4-(4-pyridinyl)-l-piperazinyl]carbonyl]pentyl]amino]-1-[(3,5-dibromo-4-hydroxyphenyl)methyl]-2-oxoethyl]-4-(1,4-dihydro-2-oxo-3(2H)-quinazolinyl) (BIBN4096BS) affinity for calcitonin gene-related peptide and amylin receptors – the role of receptor activity modifying protein 1. Mol Pharmacol 70: 1984–1991.

Higuchi R, Krummel B, Saiki RK (1988). A general method of in vitro preparation and specific mutagenesis of DNA fragments: study of protein and DNA interactions. Nucleic Acids Res 16: 7351–7367.

Hilton JM, Dowton M, Houssami S, Sexton PM (2000). Identification of key components in the irreversibility of salmon calcitonin binding to calcitonin receptors. J Endocrinol 166: 213–226.

Ho HH, Gilbert MT, Nussenzveig DR, Gershengorn MC (1999). Glycosylation is important for binding to human calcitonin receptors. Biochemistry 38: 1866–1872.

Ittner LM, Koller D, Muff R, Fischer JA, Born W (2005). The N-terminal extracellular domain 23-60 of the calcitonin receptor-like receptor in chimeras with the parathyroid hormone receptor mediates association with receptor activity-modifying protein 1. Biochemistry 44: 5749–5754.

Kusano S, Kukimoto-Niino M, Hino N, Ohsawa N, Okuda K-I, Sakamoto K *et al.* (2012). Structural basis for extracellular interactions between calcitonin receptor-like receptor and receptor activity-modifying protein 2 for adrenomedullin-specific binding. Protein Sci 21: 199–210.

Mack C, Wilson J, Athanacio J, Reynolds J, Laugero K, Guss S *et al*. (2007). Pharmacological actions of the peptide hormone amylin in the long-term regulation of food intake, food preference, and body weight. Am J Physiol Regul Integr Comp Physiol 293: R1855–R1863.

Moore EL, Gingell JJ, Kane SA, Hay DL, Salvatore CA (2010). Mapping the CGRP receptor ligand binding domain: tryptophan-84 of RAMP1 is critical for agonist and antagonist binding. Biochem Biophys Res Commun 394: 141–145.

Morfis M, Tilakaratne N, Furness SGB, Christopoulos G, Werry TD, Christopoulos A *et al*. (2008). Receptor activity-modifying proteins differentially modulate the G protein-coupling efficiency of amylin receptors. Endocrinology 149: 5423–5431.

Neubig RR, Spedding M, Kenakin T, Christopoulos A; International Union of Pharmacology Committee on Receptor Nomenclature and DrugClassification (2003). International Union of Pharmacology Committee on Receptor Nomenclature and Drug Classification. XXXVIII. Update on terms and symbols in quantitative pharmacology. Pharmacol Rev 55: 597–606.

Pham V, Wade JD, Purdue BW, Sexton PM (2004). Spatial proximity between a photolabile residue in position 19 of salmon calcitonin and the amino terminus of the human calcitonin receptor. J Biol Chem 279: 6720–6729.

Pham V, Dong M, Wade JD, Miller LJ, Morton CJ, Ng HL *et al*. (2005). Insights into interactions between the alpha-helical region of the salmon calcitonin antagonists and the human calcitonin receptor using photoaffinity labeling. J Biol Chem 280: 28610–28622.

Poyner DR, Sexton PM, Marshall I, Smith DM, Quirion R, Born W *et al*. (2002). International Union of Pharmacology. XXXII. The mammalian calcitonin gene-related peptides, adrenomedullin, amylin, and calcitonin receptors. Pharmacol Rev 54: 233–246.

Qi T, Christopoulos G, Bailey RJ, Christopoulos A, Sexton PM, Hay DL (2008). Identification of N-terminal receptor activity-modifying protein residues important for calcitonin gene-related peptide, adrenomedullin, and amylin receptor function. Mol Pharmacol 74: 1059–1071.

Sexton PM, Findlay DM, Martin TJ (1999). Calcitonin. Curr Med Chem 6: 1067–1093.

Tilakaratne N, Christopoulos G, Zumpe ET, Foord SM, Sexton PM (2000). Amylin receptor phenotypes derived from human calcitonin receptor/RAMP coexpression exhibit pharmacological differences dependent on receptor isoform and host cell environment. J Pharmacol Exp Ther 294: 61–72.

Wookey PJ, McLean CA, Hwang P, Furness SGB, Nguyen S, Kourakis A *et al*. (2012). The expression of calcitonin receptor detected in malignant cells of the brain tumour glioblastoma multiforme and functional properties in the cell line A172. Histopathology 60: 895–910.

Young AA, Gedulin B, Vine W, Percy A, Rink TJ (1995). Gastric emptying is accelerated in diabetic BB rats and is slowed by subcutaneous injections of amylin. Diabetologia 38: 642–648.

Supporting information

Additional Supporting Information may be found in the online version of this article:

Figure S1 cAMP data showing that HEK293S cells lack endogenous responses from RAMPs, CLR or CTR. If endogenous CTR was present, the introduction of RAMP1 would have resulted in a potent CGRP response.
Figure S2 Expression of mRNA encoding CTR, CLR, RAMP1, RAMP2, RAMP3 and positive controls GAPDH in HEK293S cells by RT-PCR. Lanes 2, 4, 6, 8 and 10 are positive controls for CTR, CLR, R1, R2 and R3 primers, respectively, and show bands of the predicted size. Lanes 1, 3, 5, 7 and 9 are the paired results from mRNA prepared from HEK293S cells. No products were detected. Lane 11 shows a GAPDH housekeeping gene as a positive control for the cDNA.
Table S1 Primers used for generating FLAGhRAMP constructs.
Table S2 Summary of pEC_{50}'s for pERK1/2 responses in Cos7 cells. Data were analysed by unpaired *t*-tests.
Table S3 Rank order of agonist potencies observed at $\Delta(1–47)hCT_{(a)}$, $\Delta(1–47)hAMY_{1(a)}$, $\Delta(1–47)hAMY_{3(a)}$ and their full-length receptors in Cos 7 cells and $\Delta(1–47)hCT_{(a)}$, $\Delta(1–47)hAMY_{2(a)}$ and their full-length receptors in HEK293S cells.